Supplementary Information

Topical siRNA Therapy of Diabetic-Like Wound Healing

Eva Neuhoferova, [‡ a,b] *Marek Kindermann,* [‡ c,d] *Matej Buzgo,* [e,f] *Karolina Vocetkova,* [e] *Dalibor Panek,* [g] *Petr Cigler*[*,c] and Veronika Benson*[*,a,h]

[a]Institute of Microbiology of the Czech Academy of Sciences, Videnska 1083, 142 20, Prague 4, Czechia
[b]Faculty of Science, Charles University, Hlavova 2030, Prague 2, 128 40, Czechia
[c]Institute of Organic Chemistry and Biochemistry of the Czech Academy of Sciences, Flemingovo namesti 2, 166 10, Prague 6, Czechia
[d]Department of Physical Chemistry, University of Chemistry and Technology Prague, Technicka 5, 166 28 Prague 6, Czechia
[e]Institute of Experimental Medicine of the Czech Academy of Sciences, Videnska 1083, 142 20, Prague, Czechia
[f]InoCure s.r.o., Politickych veznu 13, 100 00, Prague, Czechia
[g]Faculty of Biomedical Engineering, Czech Technical University in Prague, Namesti Sitna 3105, Kladno 2, 272 01, Czechia
[h]Technical University of Liberec, Faculty of Health Studies, Trebizskeho 1402, 46001, Liberec, Czechia
* Corresponding authors
Emails: petr.cigler@uochb.cas.cz, veronika.benson@tul.cz
‡ These authors contributed equally.

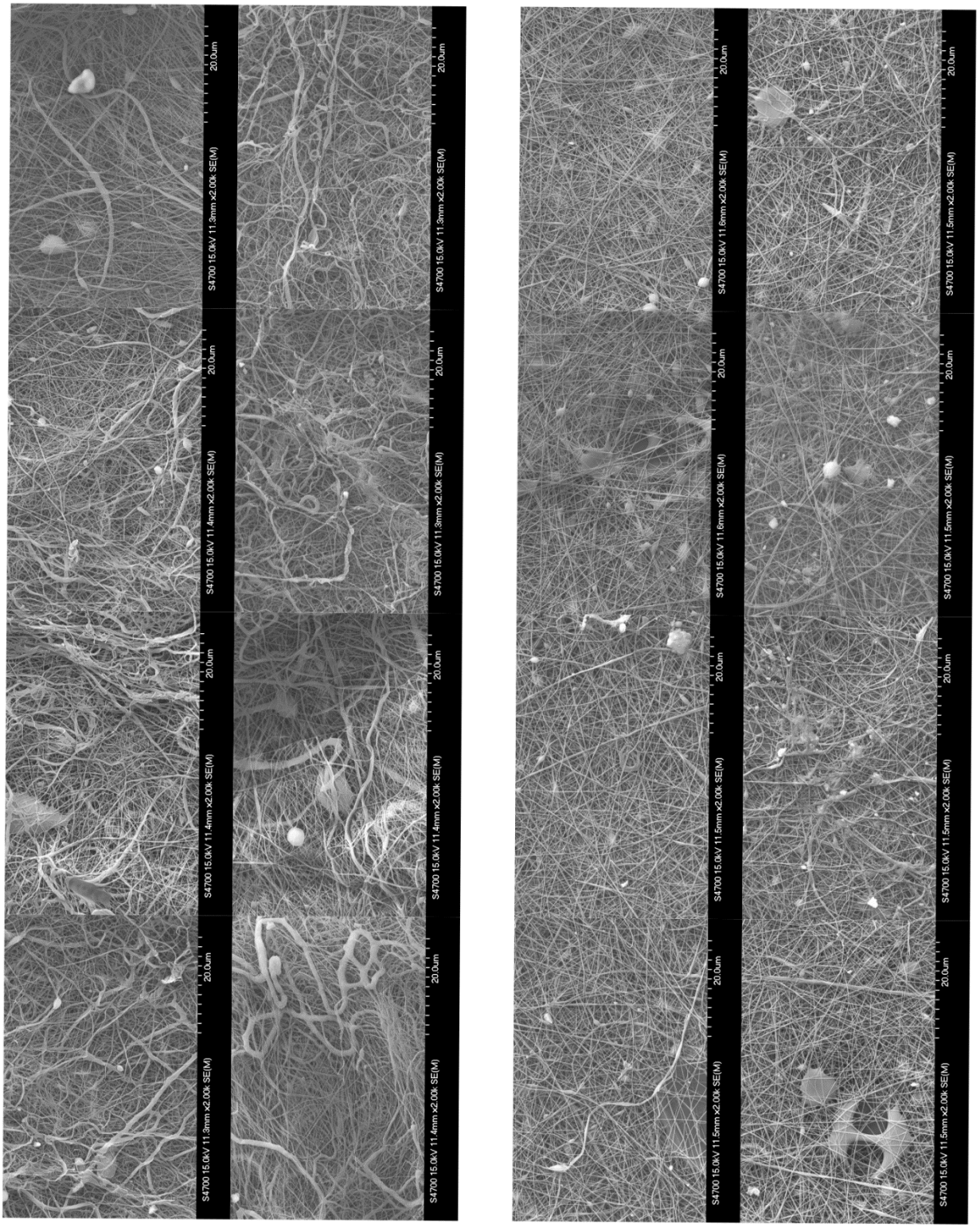

Figure S1. FESEM micrographs (only side #2) used for image analysis – **Figure 2B** – **left column:** NF{Cop^{+}-FND:siRNA}; **right column**: NF.

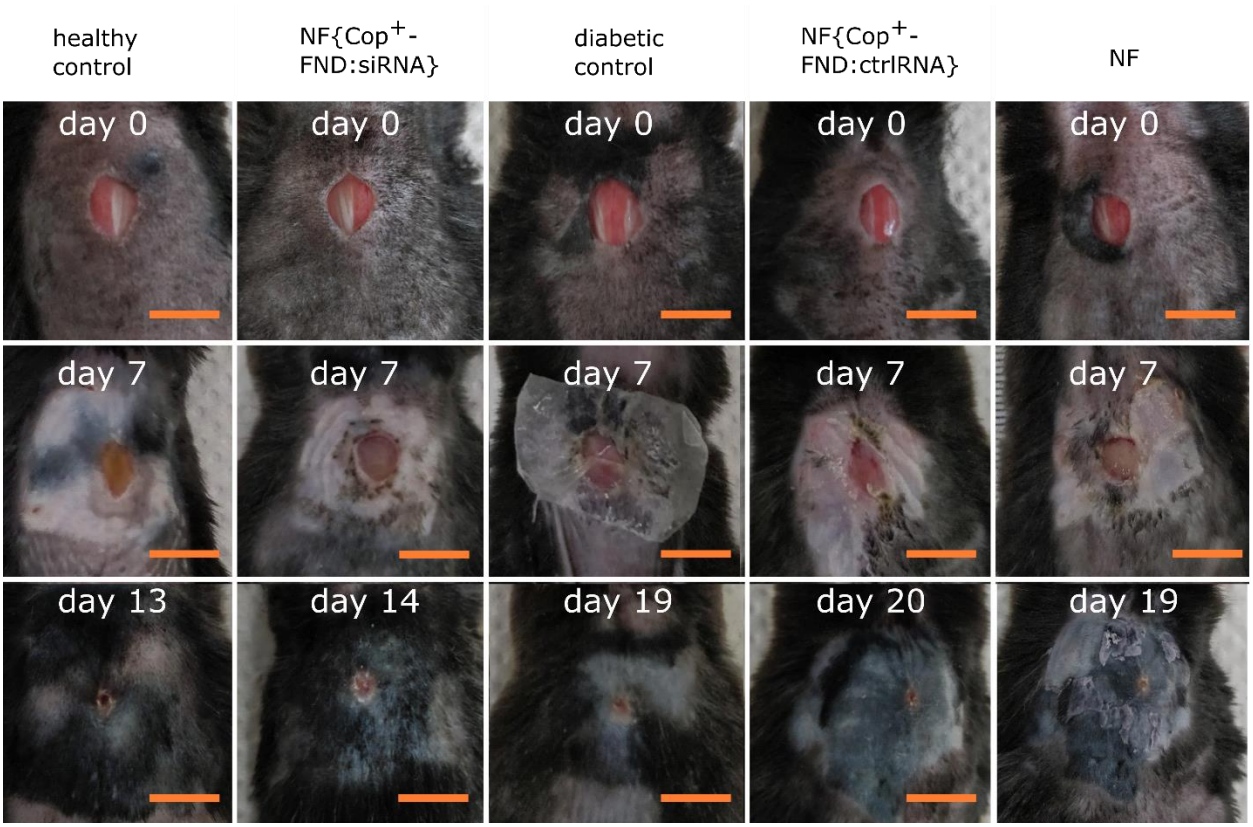

Figure S2. Group #1 – photographic representation of diabetic-like wound healing showing different rates of primary scar formation in dependence on the type of treatment. The skin condition is shown at various time points (day 0, day 7, and day of primary scar formation). Healthy and diabetic controls were treated only with Tegaderm film without the primary nanofibre dressing. The rest of the mice were treated with the nanofibre dressing covered by Tegaderm film (a secondary dressing). The photographs represent the first experimental group (Group #1 – 4 diabetic-like animals and 1 healthy control). Scale bar represents 1 cm. If absent, the original image lacked a ruler, and the scale is unknown.

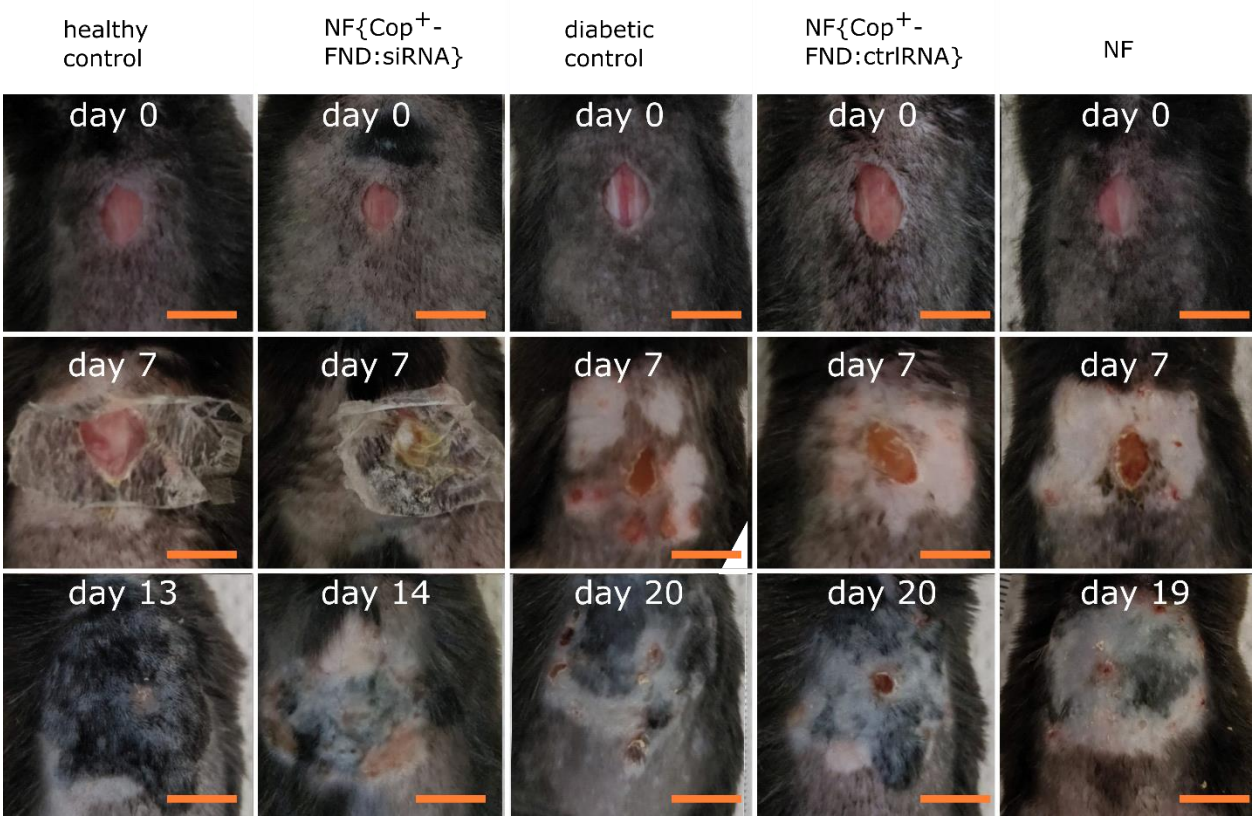

Figure S3. Group #2 – photographic representation of diabetic-like wound healing showing different rates of primary scar formation in dependence on the type of treatment. The skin condition is shown at various time points (day 0, day 7, and day of primary scar formation). Healthy and diabetic controls were treated only with Tegaderm film without the primary nanofibre dressing. The rest of the mice were treated with the nanofibre dressing covered by Tegaderm film (a secondary dressing). The photographs represent the second experimental group (Group #2 – 4 diabetic-like animals and 1 healthy control). Scale bar represents 1 cm. If absent, the original image lacked a ruler, and the scale is unknown.

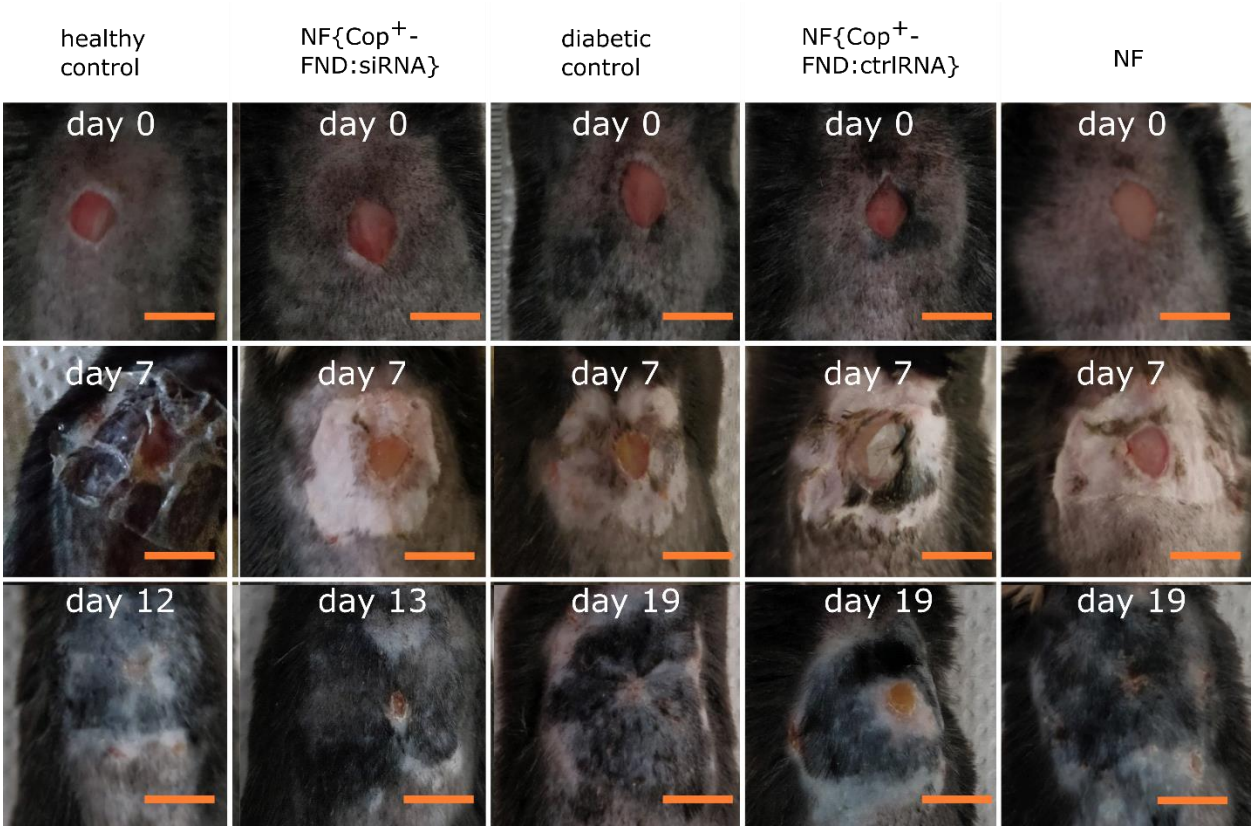

Figure S4. Group #3 – photographic representation of diabetic-like wound healing showing different rates of primary scar formation in dependence on the type of treatment. The skin condition is shown at various time points (day 0, day 7, and day of primary scar formation). Healthy and diabetic controls were treated only with Tegaderm film without the primary nanofibre dressing. The rest of the mice were treated with the nanofibre dressing covered by Tegaderm film (a secondary dressing). The photographs represent the third experimental group (Group #3 – 4 diabetic-like animals and 1 healthy control). Scale bar represents 1 cm. If absent, the original image lacked a ruler, and the scale is unknown.

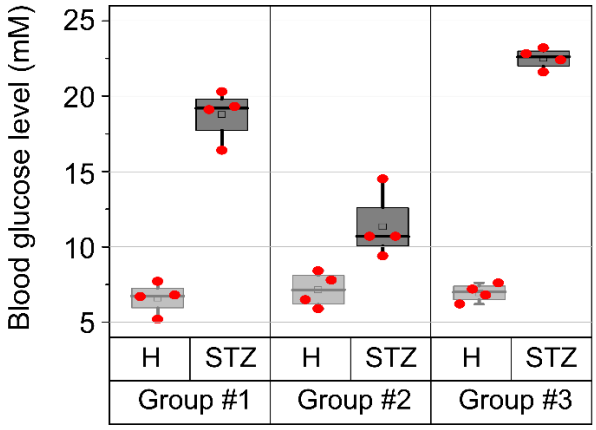

Figure S5. Raw data for blood glucose levels of healthy animals (experimental day 0; H – healthy) and the same animals after induction of diabetes-like conditions (experimental day 19; STZ – streptozotocin). Animals were divided in these groups (Group #1, Group #2, Group #3) based on the reached glucose level after the Streptozotocin treatment. See Figure 4C for the overall effect of STZ on the blood glucose level.

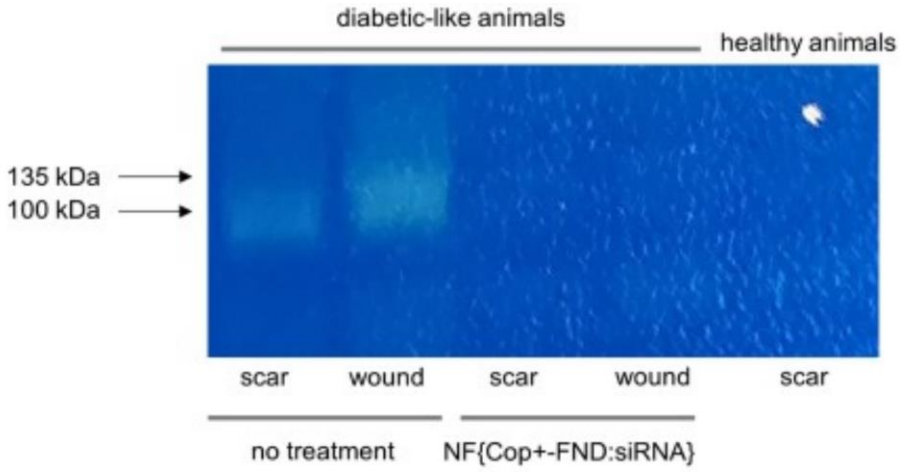

Figure S6. Activity of pre-MMP-9 and MMP-9 in wound tissues after seven days of treatment (wound; experimental day 29) in diabetic-like tissues revealed by zymography. Scar tissues from diabetic and healthy animals excised at the end of experiment are shown for comparison (scar). Precursor MMP-9 and matured MMP-9 migrated at 135 kDa and 100 kDa, respectively.

Table S1. Electrophoretic light scattering analysis of Cop^+-FND:siRNA complexes (mass ratio: ~30 : 1).

	Apparent ζ-potential [mV]	**Electrophoretic mobility [μm·cm/V·s]**	Conductivity [μS/cm]	Applied voltage [V]
Cop^+-FND:siRNA (5% PVA solution, 25 °C)	43.3 ± 2.2	3.40 ± 0.17	45.2 ± 1.1	4.98

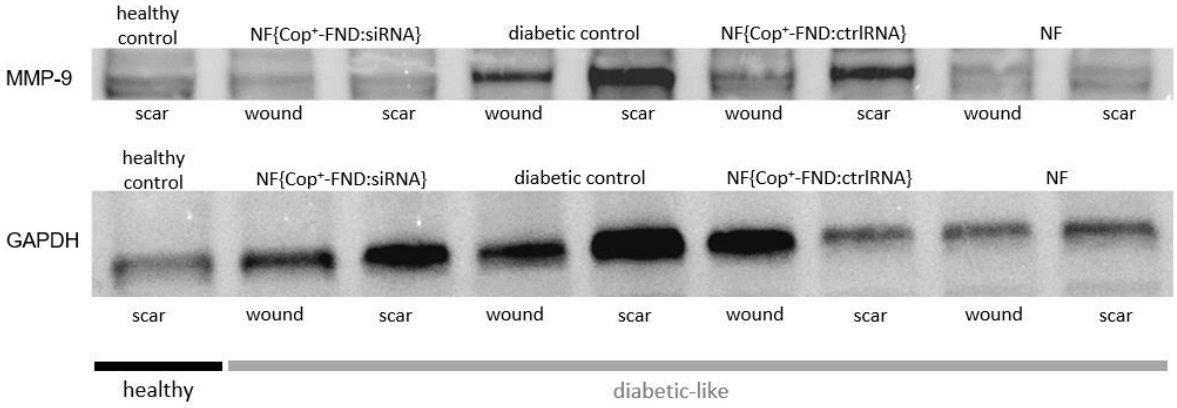

Figure S7. Level of the MMP-9 protein in excised tissues after 7 days of treatment (samples denoted as "wound") and after scar formation (denoted as "scar") in healthy and diabetic-like tissues analysed densitometrically from a Western blot – the uncropped version of the Figure 5C. For the full original image see Figures S8 and S9.

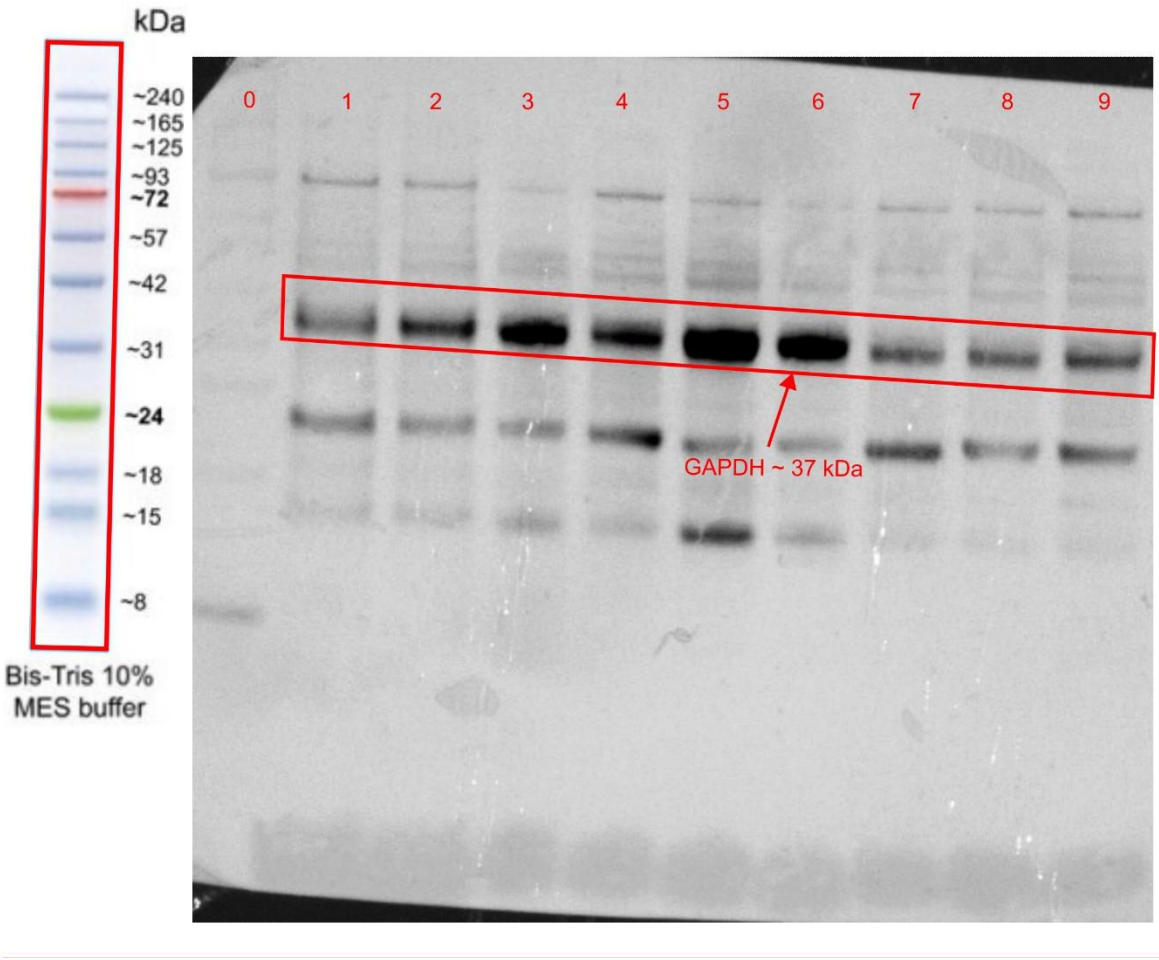

Figure S8. Original western blot image showing GAPDH protein level in excised tissues after 7 days of treatment (wound) and after scar formation (scar) in healthy and diabetic-like conditions. Lane designations: 0: protein ladder; 1: scar, healthy control; 2: wound, NF{Cop^{+}-FND:siRNA}; 3: scar, NF{Cop^{+}-FND:siRNA}; 4: wound, diabetic control; 5: scar, diabetic control; 6: wound, NF{Cop^{+}-FND:ctrlRNA}; 7: scar, NF{Cop^{+}-FND:ctrlRNA}; 8: wound, NF; 9: scar, NF.

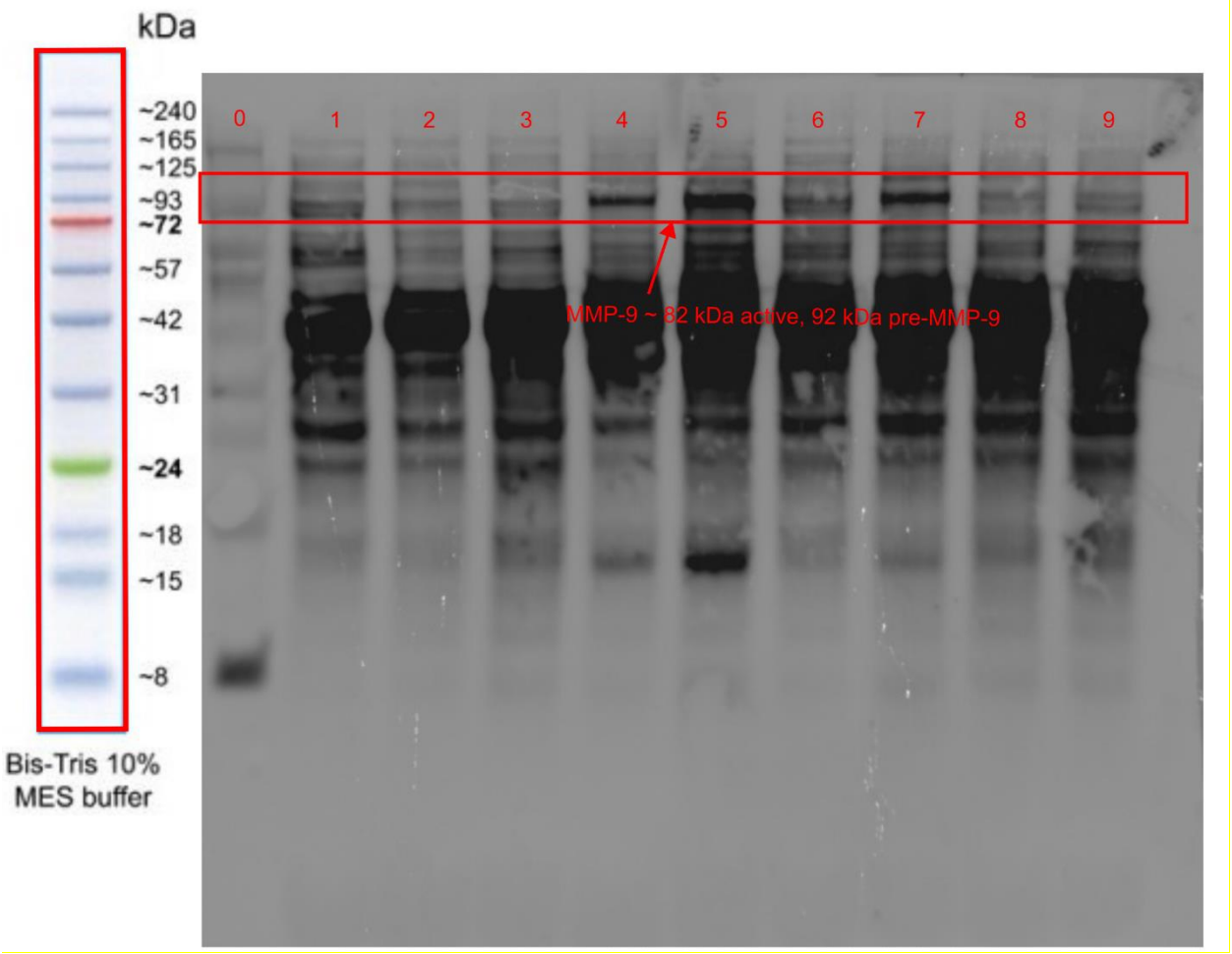

Figure S9. Original western blot image showing protein level in excised tissues after 7 days of treatment (wound) and after scar formation (scar) in healthy and diabetic-like conditions. Lane designations: 0: protein ladder; 1: scar, healthy control; 2: wound, NF{Cop^+-FND:siRNA}; 3: scar, NF{Cop^+-FND:siRNA}; 4: wound, diabetic control; 5: scar, diabetic control; 6: wound, NF{Cop^+-FND:ctrlRNA}; 7: scar, NF{Cop^+-FND:ctrlRNA}; 8: wound, NF; 9: scar, NF.

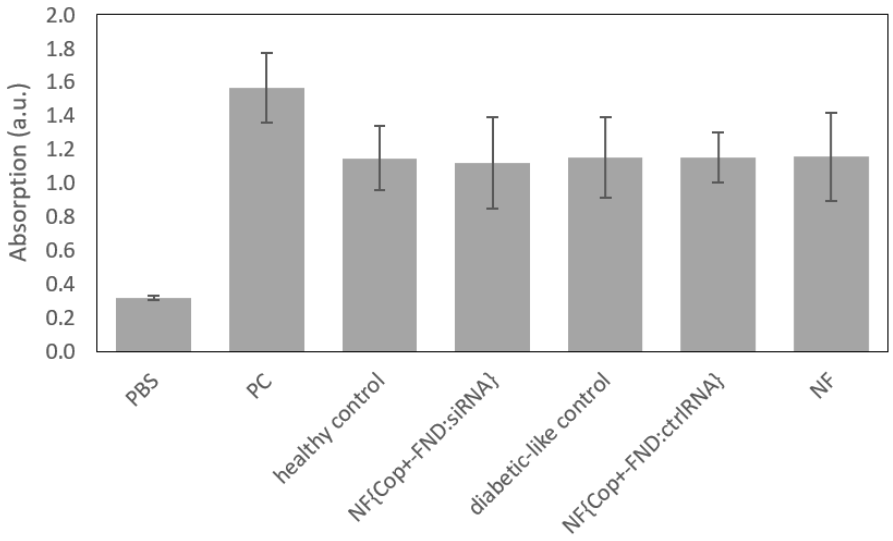

Figure S10. Serum levels of alanine aminotransferase (ALT).

Statistical analysis

Analysis of time-to-event data (Figure 5A, B) requires techniques for positive-valued random variables (survival models). As a first-choice model, we utilized the semiparametric *Cox proportional hazards model* to compare wound closure rates. This approach makes no specific assumptions about the hazard function $\boldsymbol{h(t)}$ which describes the frequency at which wound closure occurs per unit of time, given that the event has not yet happened (instantaneous wound closure). The obtained results (not shown) were strongly dependent on the choice of prior information and is therefore not very useful for further discussion. Imposing more strict assumptions on the hazard function leads to fully parametric models.[1] The basic single-parameter exponential model states that the hazard function is constant over time. This is not a very reasonable expectation for the wound closure process. This expectation would imply that a non-negligible fraction of animals would experience wound closure after a very short time after wounding (e.g. after two days). Two-parameter models bring more flexibility when concerning hazard profiles. Being aware of this, we utilized the two-parameter Weibull model, which allowed us to assume a more feasible monotonically increasing hazard function $\boldsymbol{h_W(t)}$ (see Equation 3 for $\boldsymbol{\alpha > 1}$).[2,3] In other words, the chance of wound closure increases with time. Results of the Weibull regression model in Figure 5A-B (smooth curves) are shown in terms of the survival function $\boldsymbol{S_W(t)}$ (see Equation 2), which describes the probability that wound closure has not occurred by the elapsed time.
Regarding the model limitations, the applied two-parameter form of the Weibull regression model assumes not only a monotonic profile of the hazard functions, but also their proportionality. In other words, survival curves (e.g. in Figure 5A-B) are not allowed to cross among treatments.[4] In addition, one could alternatively consider the application of a three-parameter Weibull model (a third shift parameter is included) due to the moderately large Weibull shape parameter ($\alpha = 38$) obtained by the two-parameter version.[5]

Survival analysis of the time-to-event data (time to wound closure) was performed using a Weibull regression model in a Bayesian framework (Figure 4) using software packages in R.[60–67] The

probability density function $f_W(t)$, underlying survival $S_W(t)$ and hazard $h_W(t)$ functions of Weibull random variable T were given by Equations (1)–(3):

$$f_{\mathrm{W}}(t) = \frac{\alpha}{\lambda}\left(\frac{t}{\lambda}\right)^{\alpha-1} e^{-\left(\frac{t}{\lambda}\right)^{\alpha}}, \qquad (1)$$

$$S_{\mathrm{W}}(t) = e^{-\left(\frac{t}{\lambda}\right)^{\alpha}}, \qquad (2)$$

$$h_{\mathrm{W}}(t) = \frac{\alpha}{\lambda}\left(\frac{t}{\lambda}\right)^{\alpha-1}. \qquad (3)$$

The Bayesian model defined below was fitted with the 'brms' package[65] that employs Stan software for probabilistic sampling.

$$\begin{aligned} &\text{likelihood:} && t_i \sim \mathrm{Weibull}(\lambda_i, \alpha) \\ &\text{linear model:} && \log \mu_i = \textstyle\sum_j \beta_j X_{i,j} \\ & && \lambda_i = \dfrac{\mu_i}{\Gamma(1 + 1/\alpha)} \qquad (4) \\ &\text{priors:} && \beta_j = \mathrm{Normal}(0, 2) \\ & && \alpha = \mathrm{Gamma}(0.01, 0.01) \end{aligned}$$

The first row represents the stochastic part of the model and states that the response variable T is a random variable independently drawn from a Weibull distribution with shape parameter α and scale parameter λ. The linear model in the second line describes how $\log \mu_i$ (log of the conditional mean for the response variable) is constructed for the given treatment j; $X_{i,j}$ is an indicator variable. The remaining lines describe weakly informative prior distributions. Unlike the Weibull likelihood as implemented in the 'brms' package, the linear model is parametrized in terms of $\log \mu_i$, the back-transformation of estimated β_j parameters into the λ metric was performed using Equation (4);[68] Γ is the gamma function.

References

[1] I. van Oostrum, M. Ouwens, A. Remiro-Azócar, G. Baio, M. J. Postma, E. Buskens, B. Heeg, *Value Health* **2021**, *24*, 1294.

[2] A. S. Kurz, *Statistical rethinking with brms, ggplot2, and the tidyverse: Second edition*, version 0.4.0., **2023**.

[3] Bayesian Survival Analysis of Acute Encephalitis Syndrome with Censoring Mechanism using Brms Package, *J. Stat. Appl. Probab.* **2022**, *11*, 963.

[4] H. Campbell, C. B. Dean, *Stat. Med.* **2014**, *33*, 1042.

[5] D. Cousineau, *IEEE Trans. Dielectr. Electr. Insul.* **2011**, *18*, 2095.